NANO MICRO
small

Supporting Information

for *Small,* DOI: 10.1002/smll.201703357

Reversible Immobilization of Proteins in Sensors and Solid-State Nanopores

Adithya Ananth, María Genua, Nesrine Aissaoui, Leire Díaz, Nico B. Eisele, Steffen Frey, Cees Dekker, Ralf P. Richter,* and Dirk Görlich*

Supporting Information

Reversible Immobilization of Proteins in Sensors and Solid-state Nanopores

Adithya Ananth, María Genua*, Nesrine Aissaoui*, Leire Díaz, Nico B. Eisele, Steffen Frey, Cees Dekker[$], Ralf P. Richter[$] and Dirk Görlich*

Supporting Figures

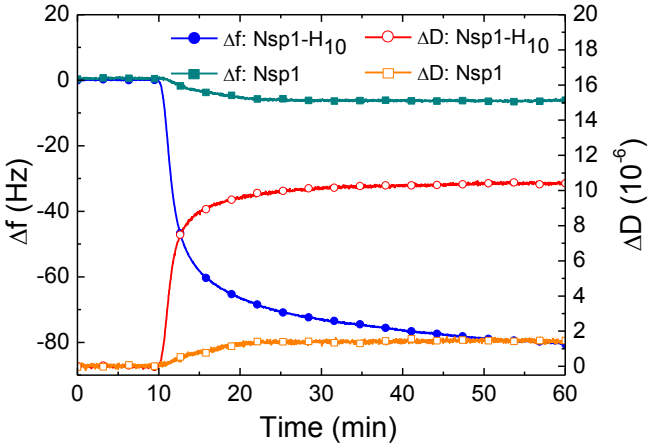

Figure S1. Selectivity for His-tagged proteins. The selective anchoring *via* the His tag was evaluated by comparing the binding of Nsp1-H_{10} with an identical Nsp1 construct that lacks the His tag. While Nsp1-H_{10} binding is comparable to Figure 2, only minor binding is observed for Nsp1. Conditions: buffer – 10 mM HEPES, 150 mM NaCl, pH 7.4; Nsp1-H_{10} and Nsp1 –1.5µM; surfaces were functionalized with EDTA and loaded with $NiCl_2$ (2 mM for 15 min) prior to the measurements.

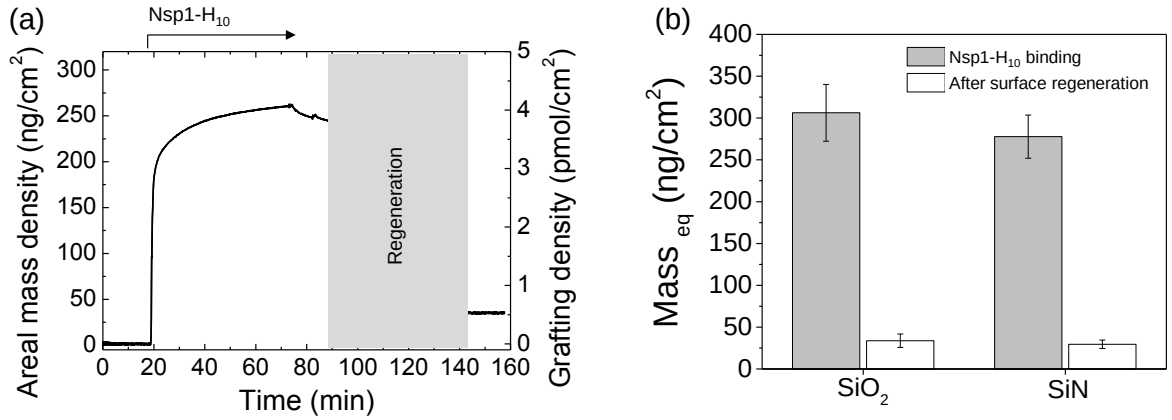

Figure S2. Functional coatings on SiN and SiO_2 have comparable propensity to immobilize His-tagged proteins. (a) SE data of Nsp1-H_{10} binding and triggered release on functionalized SiN with a solution of 0.5 M imidazole and 1 M GuHCl (for 50 min, not shown). The maximal bound amount, binding stability and specificity of binding is comparable to SiO_2 (cf. Figure 2). (b) Averaged areal mass density of immobilized Nsp1-H_{10}, measured by SE after 50 min of incubation at 1.5 µM (grey bars) and after surface regeneration as in (a) (white bars) for functionalized SiO_2 and SiN surfaces. Error bars are standard deviations of independent measurements with 8 different SiO_2 surfaces and 4 different SiN surfaces. Conditions: buffer – 10 mM HEPES, 150 mM NaCl, pH 7.4; Nsp1-H_{10}– 1.5 µM; surfaces were functionalized with EDTA and loaded with $NiCl_2$ (2 mM for 15 min) prior to the measurements.

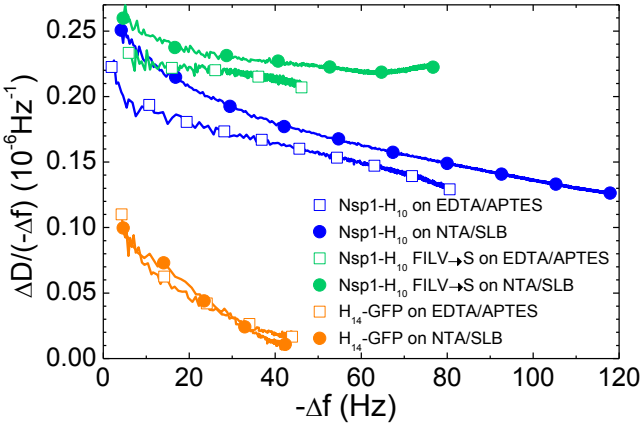

Figure S3. Morphology of protein films. The parameter $\Delta D/-\Delta f$ was derived from QCM-D data and is a measure for the softness of the protein films; $-\Delta f$ is a measure for the surface coverage. Because film mechanical properties and morphology are linked, this parametric plot provides insight into the evolution of the overall film morphology with protein coverage.[24-25] Data for proteins on Ni^{2+}-EDTA on aminosilane are taken from Fig. 4a. For comparison, data on supported lipid bilayers (SLBs) displaying Ni^{2+}-loaded nitrilotriacetic acid (Ni^{2+}-NTA) for capture of His-tagged proteins are also shown (Nsp1-H_{10} and Nsp1-H_{10} FILV→S from Fig. 4 in ref. [19d], H_{14}-GFP from Fig. 2 in ref. [24]). Proteins on aminosilane exhibit the same trends as on SLBs: Nsp1-H_{10} FILV→S films are softer than Nsp1-H_{10} films owing to the reduced cohesiveness of the mutant protein, and both films become more rigid as protein coverage increases and the films become denser. It is notable that Nsp1 FG domain films appear slightly more rigid when formed on aminosilanes as compared to SLBs. We tentatively attribute this to differences in the anchorage: when anchored to the SLBs, proteins are laterally mobile but when anchored to aminosilanes they are not. As expected, the monolayer of globular GFP appears much more rigid than the meshwork of disordered and interpenetrating Nsp1 FG domains. The rigidity of GFP films is comparable on aminosilanes and on SLBs. For GFP, the decrease in $\Delta D/-\Delta f$ with $-\Delta f$ is due to hydrodynamic coupling between proteins, as explained in detail in ref. [24].

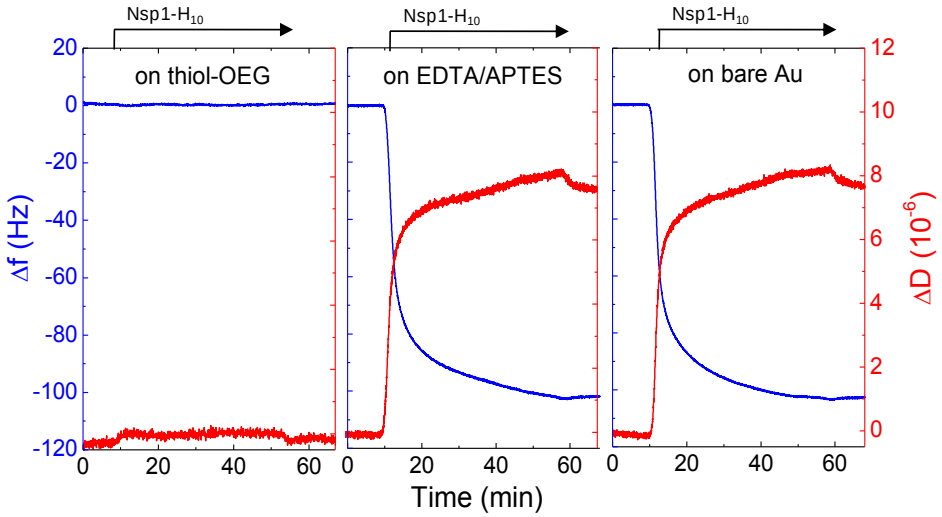

Figure S4. OEG-coated gold surfaces are inert to protein adsorption. The QCM-D shift upon exposure of Nsp1-H_{10} to differently functionalized gold surfaces: thiol-OEG, EDTA/APTES, and bare gold (as indicated). No response is observed on thiol-OEG demonstrating full passivation by comparison to the strong QCM-D shift obtained upon Nsp1-H_{10} adsorption on EDTA/APTES functionalized gold and on bare gold. Conditions: buffer – 10 mM HEPES, 150 mM NaCl, pH 7.4; Nsp1-H_{10} – 1.5 µM.

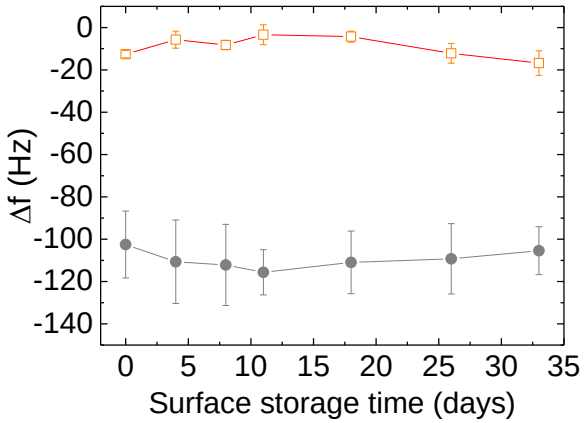

Figure S5. Stability upon storage and re-use of orthogonally functionalized surfaces. QCM-D frequency shifts at equilibrium, upon incubation with a His tagged FG domain H_{18}-Mac98 (0.3 µM for 60 min) are shown as a function of storage time. This reflects the conservation of His-tag binding capacity on silica (grey filled circles) and the passivation of gold (orange open squares) over the course of one month. Before each measurement, the surfaces were re-loaded with $NiCl_2$; after each measurement, the surfaces were regenerated with 0.5 M imidazole and 1 M GuHCl (30 min), rinsed with buffer and water, blow-dried in nitrogen gas and stored dry in the dark at room temperature until the next measurement. Error bars represent standard deviations for two measurements with two different sensors; the same sensors were repeatedly used to acquire all data shown. For this set of measurements, the FG domain of Nup98 from *Tetrahymena thermophila* with an N terminal H_{18} tag (H_{18}-Nup98; 61 kDa; see B. Schmidt, D. Görlich. *eLife.* **2015,** *4*, e04251 for protein preparation) was used thus demonstrating application to another His tagged protein. Additional tests with Nsp1-H_{10} over a period of 20 days showed comparable stability.

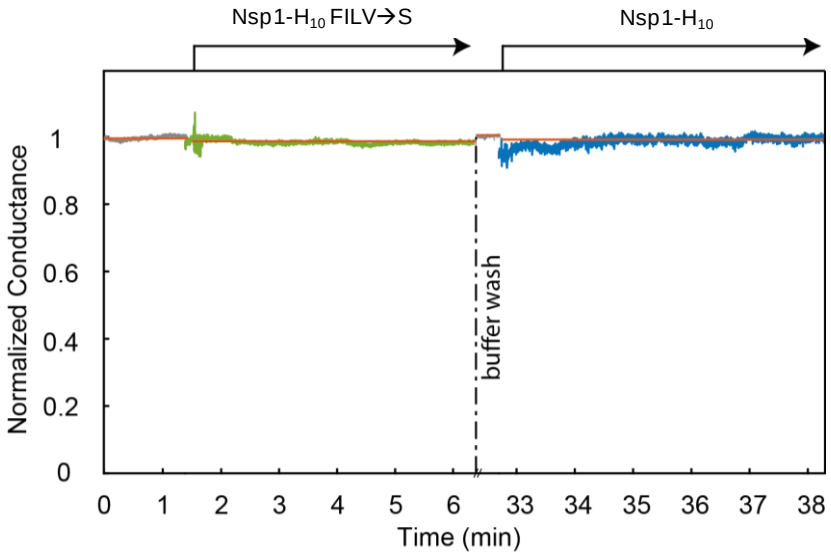

Figure S6. Nsp1-H_{10} proteins do not bind to bare SiN nanopores. Representative ion current traces for bare SiN nanopores of 40 nm diameter. Exposure to Nsp1-H_{10} and Nsp1-H_{10} FILV→S (as indicated) does not affect the conductance level significantly compared to the baseline conductance. Data are presented analogous to Figure 6a. Across triplicates of the set of injections shown, currents changed by less than 5% compared to baseline.

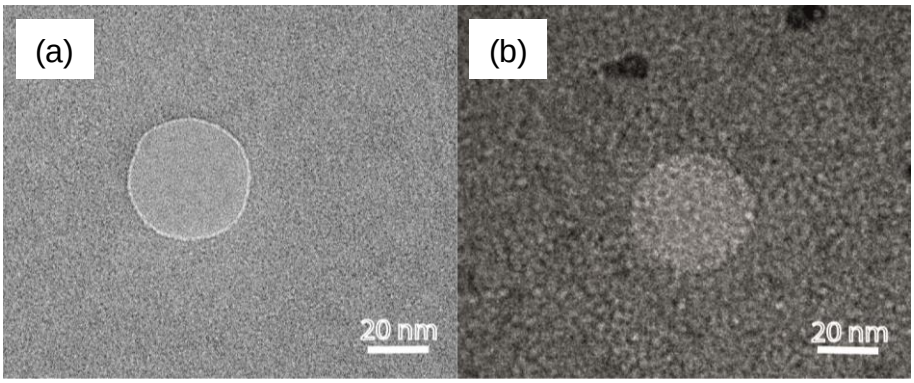

Figure S7. Transmission electron micrographs of nanopores. (a) Bare nanopore of 40 nm diameter. (b) The same nanopore after *in situ* Nsp1-H_{10} coating. In (b), the presence of bio-organic material in the pore and on the SiN membrane surface is evidenced by the grainy appearance which is lacking in (a). Similar images have been reported in a previous study for Nsp1-coated solid-state nanopores.[18c] We emphasize that the exact structural arrangement of the Nsp1 cannot be elucidated from such images because the structure of disordered proteins is generally difficult to resolve, and because the sample has been dried and is imaged in high-vacuum imaging conditions.

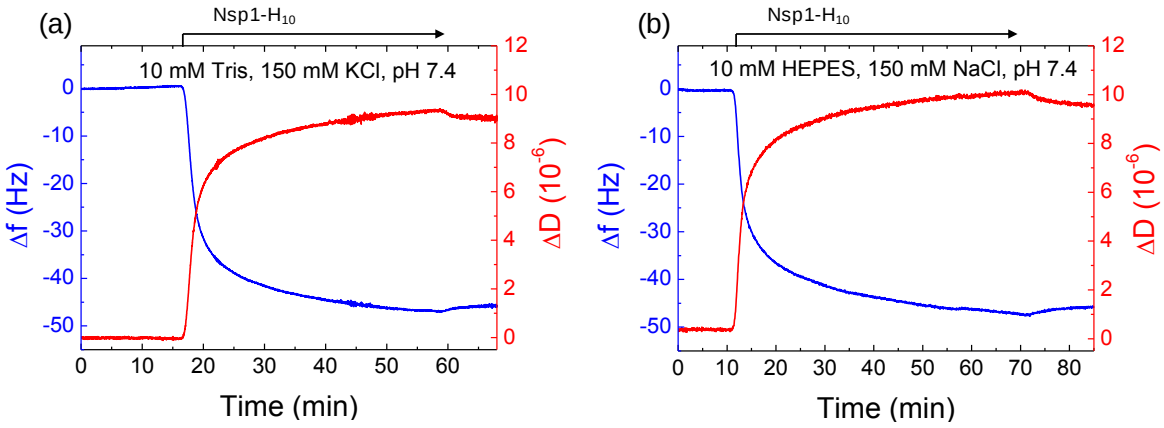

Figure S8. Buffer and cation types do not affect Nsp1 immobilization. Binding of Nsp1-H_{10} FILV→S is shown in (a) 10 mM Tris, 150 mM KCl, and in (b) 10 mM HEPES, 150 mM NaCl, both at pH 7.4. Conditions: Nsp1-H_{10} – 1.5 μM; silica surfaces were functionalized with EDTA and loaded with $NiCl_2$ (2 mM for 15 min) prior to the measurements.